Chapter

Principles and Applications of Nanoplasmonics in Biological and Chemical Sensing: A Review

Parsoua A. Sohi and Mojtaba Kahrizi

Abstract

Biosensing requires a highly sensitive real-time detection of the biomolecules. These properties are granted by nanoplasmonic sensing techniques. SPR-based optical sensors have evolved as a sensitive and versatile biosensing tool. A growing number of SPR-based sensing applications in the solution of clinical problems are reported in the recent years. This refers to the point that these sensors provide label-free detection of the living cells and non-destructive analysis techniques. In this study, we will review the mechanism of the detection in SPR biosensing, followed by the methods used to develop sensors to detect gases and the chemical, biological, and molecular interaction. The device sensitivity improvement based on plasmonic effects is also addressed in this study, and accordingly, the size and material dependence of the resonance frequency are discussed. The reviewed articles are categorized into three groups, depending on the SPR excitation configuration. In the first group of the sensors, the sensitivity of LSPR-based sensors in prism coupler configurations is reviewed. The second group, SPR excitation by optical fiber, slightly improved the sensitivity of the detections. The unique capability of the third group, photonic crystal fiber SPR sensors, in providing greatly improved sensitivity, generated a vast field of researches and applications in biosensing devices.

Keywords: surface plasmon resonance, localized surface plasmon resonance, nanoplasmonics, biosensors, extraordinary optical transmission, photonic crystals

1. Introduction

For the measurements of chemical and biological quantities in biomedical applications, a variety of methods were available and researched extensively in the last 30 years. In optical sensing, the first chemical sensors were based on the absorption spectrum of species to be measured [1]. Other chemical and biosensors have been developed since that time based on a diversity of optical techniques that involved luminescence, phosphorescence, fluorescence, particle light scattering, Raman scattering, ellipsometry, interferometry, and surface plasmon phenomena. For sensing purposes, measurements of the refractive index and absorbance or fluorescence properties of analyte molecules or a chemo-optical transducing medium were performed using those devices.

Among the different techniques developed, the potential of surface plasmon (SP) sensors was clearly recognized due to their great sensitivity, their simple structure,

and their capacity in terms of real-time analysis of biospecific interactions without the use of labeled molecules. In fact, SP sensors have been the preferred devices used in real-time analysis situations. They are based on surface plasmon resonance, or collective electron oscillations, that may exist at a metal-dielectric interface. Light is used for excitation of the SP waves, resulting in the transfer of energy into the SP wave. As there is a strong concentration of the electromagnetic field in the dielectric, the propagation constant of the SP wave depends strongly on variations of the optical properties of the dielectric medium surrounding the metallic surface.

Light incident on a smooth metallic surface cannot excite surface plasmons due to the transverse character of the optical wave and the longitudinal character of the SP wave, preventing the coupling between the two. A coupling mechanism is thus necessary, and it can be provided by surface rugosity [2], a grating structure [3], or Kretschmann and Otto prism configurations [4, 5]. Based on this, we can classify the sensors according to the following: (a) sensors using optical prism couplers [4], (b) sensors using grating couplers [6], (c) sensors using optical fibers (SP resonance active metal layer deposited around the fiber core) [7, 8], and (d) sensors using integrated optical waveguides [9]. The sensor characteristics include (a) its sensitivity (derivative of the monitored SP resonance parameter, such as the resonant angle or the wavelength, with respect to the parameter to be determined, such as the refractive index or the overlayer thickness), (b) its resolution (minimum change in the parameter to be determined), and (c) its operating range (range of values of the parameter to be determined). As an example, resolution in the range of 4×10^{-5} refractive index unit (RIU) can be generally achieved in sensors using optical prism couplers, while sensors using grating couplers can demonstrate a resolution in the range of 10^{-6} RIU. Among existing sensing devices, SP sensors using optical fibers presented the best prospect for miniaturization, but it is no longer the case as can be seen below. For their part, sensors based on integrated optical waveguides are promising in the development of multichannel sensing devices, with however limitations on sensitivity performance due to the relatively low concentration of the electromagnetic field achieved in the analyte.

Recently, however, the event of ordered periodic nanostructures as well as of photonic crystal configurations has opened a wealth of new opportunities. Although nanoparticles are not new, new tools for their engineering in complex architectures at nanoscale have helped to discover and understand new and exciting phenomena, important not only for fundamental studies but also for device and system. Due to the renewed interest generated by the new fabrication tools (self-assembly methods, electron-beam lithographic methods, nanoimprint methods) and the extraordinary properties exhibited by ordered structures, a new term, "plasmonics," has been coined to describe the study of metallic and metallodielectric nanostructures and plasmon. The promise of highly integrated optical devices with structural elements smaller than the light wavelength made many to refer to it as the "next big thing" in nanotechnology.

2. Principle of operation

Surface plasmon is a charge density wave that exists at the interface between a metal and a dielectric. Surface plasmon polaritons (SPP) is collective oscillation of SPs, which is induced by an electromagnetic wave. This is the interesting optical property of noble metals, as these materials provide the best evidence of SPPs due to possession of high density of electrons free to move. SPs are optically excited at resonance condition. The resonance condition is referred to the condition where the momentum and energy of an incident photon matches that of a SP. Light energy can

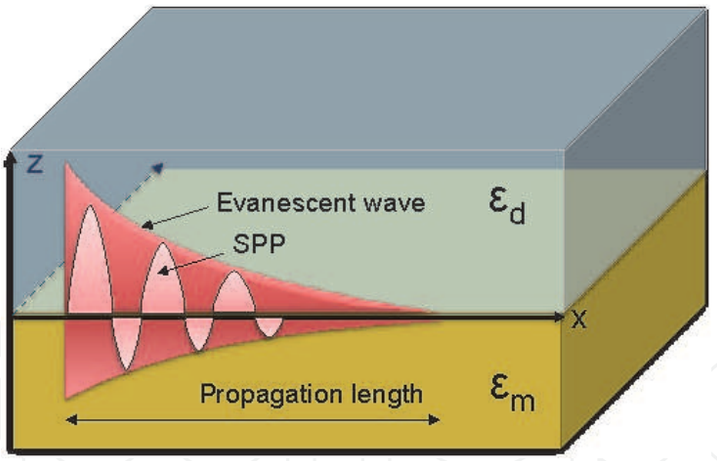

Figure 1.
SPR electromagnetic wave propagates parallel to the metal-dielectric interface. The evanescent field of SPPs is decaying in either side of the interface.

then be coupled to a SP wave which results in a strong absorption at a certain wavelength and angle of incidence. Accordingly there are two types of resonance measurement techniques: angular interrogations (measuring absorption as a function of incident angle) and wavelength interrogations (measuring absorption as a function of incident wavelength) [10, 11].

Surface plasmon resonance (SPR) can be seen as the electromagnetic surface waves that are the solution of Maxwell equation. According to the solution of Maxwell equation, SPR occurs at the interface of a material with a positive dielectric constant with that of a negative dielectric constant (such as noble metals). The waves propagate in the x-y plane along the metal-dielectric interface, and their lateral extensions evanescently decay into both sides of the interface (decay in the z-direction). The penetration length of the evanescent waves is longer for the dielectric medium compared to the metallic side (**Figure 1**).

S-polarized light (TE polarization) is referred to the polarization state that the electric field is parallel to the surface of the interface. P-polarized (TM polarized) light is the light that the electric field lays on the plane of the incident (the perpendicular plane to the surface of the interface and contains the wavevector of the excitation source). To excite the SPP modes, it is required to have the components of the electric field acting along the metal-dielectric interface. Hence, the oblique incident of the P-polarized light, which has the nonzero perpendicular electric vector component on the z-axis, is required.

P-polarized light with a particular wavelength and incident angle induces SPR once the wavevector value of the SP wave is identical to that of the incident light. The dispersion relation of the SPPs can be derived from the solution of wave equation for a P-polarized electromagnetic incident light governed by Maxwell equations subjected to the continuity of the tangential and normal field component as the boundary conditions. The wavevector of the SPP (K_{SPP}) is determined by the following relation:

$$K_{SPP} = \frac{\omega}{c}\sqrt{\frac{\varepsilon_m \varepsilon_d}{\varepsilon_m + \varepsilon_d}} \tag{1}$$

where ω is the frequency of excitation source, c is velocity of the light, and ε_m and ε_d are dielectric constants of the metal and dielectric material, respectively [12]. As the real part of the K_{SPP} for noble metals always falls below the wavevector of the

incident light $\left(K_x = \frac{2\pi}{\lambda} sin\theta\right)$, to match the wave vectors, specific excitation configuration is required. The prism coupling is a simple and standard technique to induce SPR. The underlying principle of this is to bring down the wavevector of the incident light by passing through a high refractive index prism with $n_{prism} > n_{dielectric}$ in a specific incident angle (θ). The wavevector matching at resonance condition for the prism coupler configuration is defined by

$$K_x = K_{SPP} \tag{2}$$

$$\frac{2\pi}{\lambda} n_{prism} \sin\theta = \frac{2\pi}{\lambda} \; Re\left\{\sqrt{\frac{\varepsilon_m \varepsilon_d}{\varepsilon_m + \varepsilon_d}}\right\} \tag{3}$$

where λ is the wavelength of the incident light [10]. Equation (3) states that as the refractive index of the dielectric is altered, the propagation constant of the SP mode is altered. This results in changing the coupling conditions between the incident light and SP modes.

Figure 2 demonstrates the SPR experimental setup using Kretschmann prism coupling [13, 14], which provides proper synchronization between K_{SPP} and K_x. **Figure 2b** shows the dispersion relation for SP in matter. It is seen that by using the prism, it is possible to couple the wavevectors of the SP with that of the incident light.

There are other SPR excitation configurations reported in the literature such as Otto prism coupler [15], waveguide and fiber-optic coupler [16], and diffraction grating [6]. The principal of the waveguide (and fiber-optics) coupler is close to what was explained for prism coupler, except in this configuration it is not possible to interrogate the incident angle (**Figure 3a**). In diffraction grating configuration, the incident electromagnetic radiation is directed toward a medium whose surface has a spatial periodicity (Λ) similar to the wavelength of the radiation. The incident beam is diffracted in different orders producing propagating evanescent modes at the interface. The evanescent modes have wavevectors parallel to the interface similar to the incident radiation but with integer "quanta" of the grating wavevector added or subtracted from it. These modes couple to SP, which run along the interface between the grating and the ambient medium. The diffraction grating is the only configuration that generates the SP in the same side of the metallic layer as the incident light. The only drawback of this configuration is having more than one peak in the resonance spectrum as there are several orders of diffractions in the reflected beam [17].

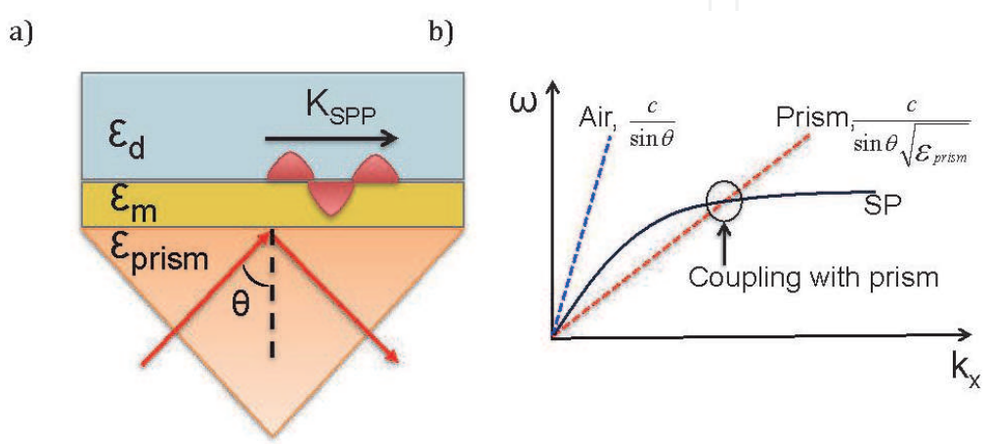

Figure 2.
(a) Prism coupling, Kretschmann configuration, and (b) dispersion relation of incident light coupling SP.

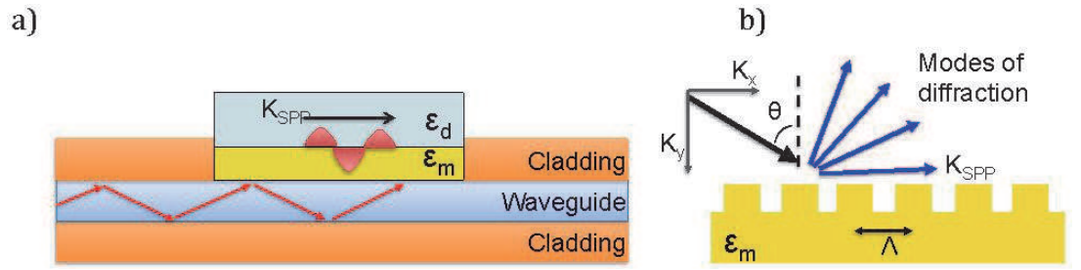

Figure 3.
(a) Waveguide coupler and (b) diffraction grating.

In the last many years, numerous researches have involved coupling photons to surface plasmons to study the effect of various materials, structure, and configurations on resonance spectrum. Potential applications extend to new light sources, solar cells, holography, Raman spectroscopy, microscopy, and sensors. In the following sections, the recent advances of SPR sensing applications are explored.

3. Applications in biological and chemical sensing

Numerous useful strategies of protein labeling have been developed for biophysical characterization of proteins including their structure, folding, and interaction with other proteins [18]. Molecular labels, such as biotin, reporter enzymes, fluorophores, and radioactive isotopes, attach covalently to target protein and nucleotides to facilitate identifying and quantifying of labeled target [19]. As the use of the molecular labels may modify the structural configuration and the binding properties of the molecules of interest, a variety of label-free methods have been developed. Among the various sensing methodologies, the SPR-based system is a reliable type of label-free technique for monitoring biomolecular interactions particularly in thermodynamic and kinetic analyses [18–21]. Biosensing application of SPR was first reported in 1983 [22, 23]. As it was mentioned in Section 2, SPR sensors are sensitive to changes in refractive index of the bulk solution in the vicinity of their active surface. Although several techniques are proposed to improve the sensitivity of SPR measurements [5, 24], the sensitivity to monolayers or molecular binding is obtained by the confinement of the plasmonic field in the nanostructured noble metals, which is known as LSPR. The smaller decay length associated with LSPR than that of SPR makes it more sensitive to local refractive index surrounding the nanostructures. **Figure 4a** illustrates the sensitivity of the LSPR spectrum of the functionalized gold nanostructures (shown in **Figure 4b**) toward adsorption of amyloid β-derived diffusible ligands (ADDL).

The impact of the shape and size of the nanostructured noble metals on the device sensitivity is demonstrated by many research groups. Analytical studies revealed that the sharp-tipped structures are reinforcing higher refractive index sensitivity due to the higher electromagnetic fields produced on their sharp edges. Reportedly, particles with sharp tips produce much higher refractive index sensitivities that would be predicted from their aspect ratios alone [12, 26–28].

Several geometries have been widely explored in recent years for developing LSPR sensors. Ekinci et al. [29] compared the extinctions spectra of Au, Al, and Ag nanoparticles of the same size. Well-defined ordered nanoparticle arrays were fabricated on quartz substrates. The diameter of the structures varied between 20 and 140 nm. Al nanoparticles with 40 nm diameters exhibit strong and sharp plasmon resonances in the near- and deep-UV ranges. Peaks in visible range were

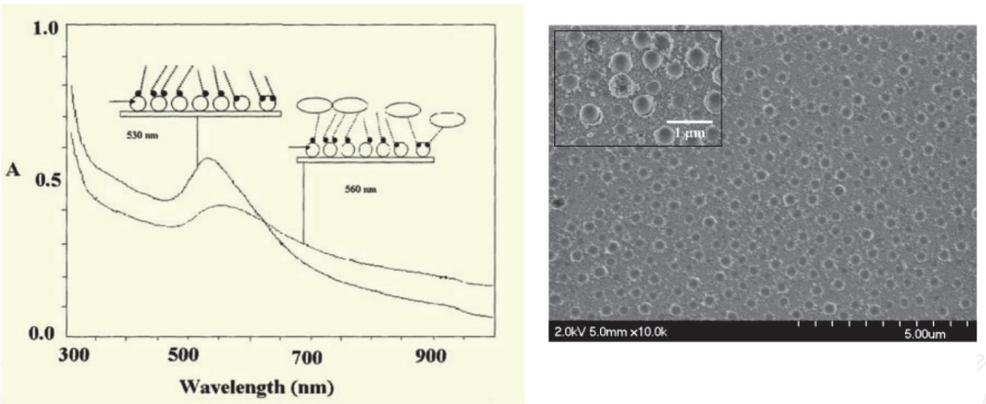

Figure 4.
(a) UV-VIS spectrum of ADDLs on gold and (b) nanohole/nanoring array prepared with 530 nm polystyrene (PSo microspheres) and 20 nm Au layer. The inset shows enlarged image of a region where PS spheres were not completely removed. Au nanoparticles are around and on the top of the spheres [25].

observed for Ag and Au nanoparticles. Increasing the diameter of the nanoparticles for tested materials resulted in a red shift in the peak position.

Considering the feasibility of fabrication, nanoring and nanodisk structures have gained great interest for their biological and chemical sensing properties. Larsson et al. [30] compared the LSPR resonance sensitivity of gold nanorings and nanodisks to refractive index changes of bulk and thin dielectric films with different thicknesses. The sensitivity of nanoring structures was found significantly higher than that of nanodisks with similar diameters in the near-infrared spectrum. Tuning of the LSPR peak wavelength between approximately 1000–1300 nm was obtained by changing the diameter of the nanorings. It is also reported that the extinction spectrum [31] of the nanoring structure is affected by the angle of incidence. By varying the incidence angle from normal to oblique, several higher-energy plasmon resonances appear in the extinction spectrum of the nanoring structures [32].

The mechanism of the enhancement of plasmon resonance in a ring array is analytically studied by Wang et al. [33]. They successfully studied the sensitivity of the device based on the dimension and periodicity of the nanorings. According to their results, increasing the thickness of the nanorings introduces a blue shift in resonance peak wavelength. For the thicknesses above 40 nm, the second resonant peak appears near the short wavelength (below 600 nm). Regarding the periodicity, as the period decreases, a red shift was observed in the position of resonance peak. Sensing characteristics of the optimum sensor was experimentally tested for refractive indices in the range of 1.33–1.4 (obtained from different ratios of glycerol water mixtures). The results also showed a linear relationship of the peak position and refractive index of the medium.

Although biological sensing applications of nanostructure-based LSPR have been reported in several laboratory level studies, commercialized implementation of this technique still requires large improvement regarding reproducibility of the structures in terms of size and shape of nanoparticles. Reproducible structures such as patterned thin films either with perforations or protrusions show a similar plasmonic response [34].

Parsons et al. [35] compared the plasmonic response of nanoparticle and nanohole arrays. They have shown that the spectral response depends on inter-hole separation, while there seems to be little effect of the interparticle spacing. This conclusion is referred to the coupling mechanism of the SPP mode that the thin metal film supports. It was also shown that the resonant spectrum of the thin film perforated with nanohole arrays is qualitatively similar to a particle of approximately the same dimensions and quantitatively shows weaker local field

enhancements. Conclusively, in general, LSPR of nanoparticles is more suitable for applications which rely on large local enhancements of electric field, such as surface enhanced Raman scattering.

Another form of SPR-based sensors involves extraordinary light transmission (EOT). Periodic structures consisting of a thin metallic film perforated with an array of nanoscale holes exhibit EOT provided that the hole size is in the subwavelength range. This porous structure can convert light into SPs by providing the necessary momentum conservation for the coupling process. EOT is determined when the transmission spectrum contains a set of peaks with enhanced transmission, although the individual holes are so small that they do not allow propagation of light. Multiple EOT peaks are correlated with excitation of various SPP modes. These peaks are generated by excitation of LSP modes which occurs in the inner

Structure	Study*	Sensitivity (nm/RIU)	Range of λ	Medium/ RI	Comment	Ref
Au nanoring	Experimental	880	NIR	1.33–1.4	LSPR. Effect of size is studied	[30]
Double split Au nanoring	Analytical	1200	NIR	1.33–1.38	LSPR. Effect of ring configuration is studied	[43]
Au nanowell	Experimental	1200–1600	Vis-NIR	1–1.6	LSPR. Tuned based on geometrical parameters	[44]
Au thin film with cubic nanoholes	Analytical	2000	Vis	1.333 and 1.357	LSPR. In this study protrusive thin films showed higher sensitivity	[10]
Au thin film with circular nanoholes	Experimental	300	Vis	1.333–1.35	LSPR. Dielectric spacer layer between plasmonic film and substrate improved the sensitivity	[45]
Au thin film with circular nanoholes	Experimental	200	Vis-NIR	1–1.5	LSPR. The resonance peak was tuned from 650 to 850 nm by varying the interhole separation	[46]
Au nanoparticle	Experimental	57	UV-Vis	1–1.658	LSPR. Nonuniform structures. Particles with mean diameters of 18 ± 2 nm	[47]
Au nanoring	Experimental	—	UV-Vis	ADDL fibrinogen AT5G0701	LSPR	[25]
Quantum dots of copper sulfate	Experimental	—	NIR	1.46, 1.51, 1.63	LSPR, refractive indices refer to CCl4, TCE, and CS2	[48]
Au colloidal nanoparticles	Experimental	70	Vis	1.32–1.5	LSPR, 30 nm diameter of the particles	[49]
Au thin film with nanoholes	Experimental	481	Vis-NIR	1.33–1.36	EOT, holes of 200 nm diameter with 500 nm periodicity	[50]
Au nanorods	Experimental	650	NIR	1.34–1.7	LSPR, tunable with size of the particles	[51]

**In most reported researches, analytically studied sensors show higher sensitivities than that of the experimental studies.*

Table 1.
Characteristics of several reported SPR-based biological/chemical sensors.

surface of hole arrays and SPP modes at the surface of the thin film, in the upper and lower rims of the holes [36].

The transmission of electromagnetic waves through a subwavelength hole was investigated by Bethe [37] for the first time. The transmission will occur at specific frequencies imposed by geometrical parameters of the structure, polarization, angle of incident light, and permittivity of the surrounding media. These findings found many applications owing to the simplicity with which their spectral properties can be tuned on.

In several studies [38–41] it was shown that the peak positions are determined by the periodicity of the holes. The periodicity is usually comparable to the wavelength of the incident light. By modifying the film thickness and diameter of the holes, one can control the shape of the peaks in terms of the width and intensity. It was due to these facts that many researchers believe that SPP is responsible for EOT and developed models to explain the phenomena.

The simple structure (perforated thin films) of EOT-based devices is widely studied for potential applications, from optical switches and photolithography masks to sensing applications. Despite this simple structure, the quality of the noble metal film in terms of surface roughness, grain size, and purity is equally important for EOT device application. A single crystalline thin film with atomically smooth surface is required in order to maximize the propagation length of SPP. A smooth surface results in elimination of scattering and loss of the incident light. This improves the transmission spectrum of the device, though it is very challenging to synthesize or grow uniform single crystalline films over a large area [42].

Table 1 summarizes the reported characteristics of few SPR-, LSPR-, and EOT-supported sensors. As it can be seen, the geometry of the metal film plays an important role in plasmon frequency. As an example, gold has plasmon frequency in the deep ultraviolet; however geometric factors create the possibility to tune the resonance peak wavelength range. The sensitivity (S) of the sensors utilizing the wavelength interrogation is defined as

$$S\left(\frac{nm}{RIU}\right) = \frac{\delta\lambda_{res}}{\delta n_d} \tag{4}$$

where $\delta\lambda_{res}$ is the offset of the resonance peak and δn_d is the change in the refractive index of the dielectric medium.

4. SPR sensitivity improvements using photonic crystal fiber

As mentioned in previous sections, the conventional prism-based Kretschmann setup is widely used for SPR sensors. However, this configuration is bulky due to the required optical measurement components. Furthermore, this configuration is not adequate for remote sensing [7]. The remarked limitations of conventional SPR configurations led to the use of optical fiber instead of the prism. Chemical sensing application of optical fiber configuration was proposed by Jorgenson et al. [52, 53] for the first time, and since then the advantages of various configurations of optical fiber based SPR sensors have drawn a lot of attention. Sensing properties of numerous microstructure optical fiber (MOF)-based SPR have been reported in the last two decades. The sensing properties of some of these sensors are summarized in **Table 2**.

Further improvement in terms of sensitivity and resolution is obtained by photonic crystal fiber-based SPR (PCF SPR). PCFs are similar to conventional optical fiber, but with periodic air holes inside the cladding region. The diameter of the air

Structure	Study	Sensitivity (nm/RIU)	Range of λ	Medium/ RI	Comment	Ref
Single mode, Au-coated core	Experimental	3200	Vis	1.33–1.3385	The sensor is able to detect index changes as low as 4×10^{-6} under moderate fiber deformations	[57]
Tapered fiber, Au-coated	Experimental	400	Vis-NIR	1.35–1.42	The sensor provides qualitative and quantitative biochemical detection	[58]
Biconical tapered, Au-coated	Experimental	2100	Vis	1.326–1.375	—	[59]
Uncladded fiber, Au-coated	Experimental	1700	Vis-NIR	1.333–1.35	Red shift was observed in resonance wavelength of the patterned Au layer	[60]

Table 2.
Characteristics of several reported fiber-optic SPR-based sensors.

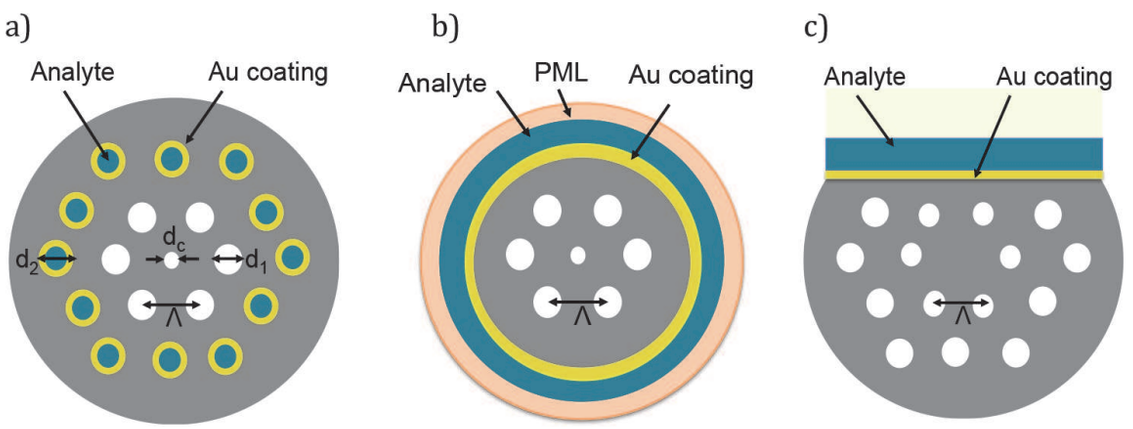

Figure 5.
Schematics of PCF-SPR sensors. (a) Analyte-filled cladding holes [54], (b) externally coated PCF [55], and (c) D-shaped PCF SPR sensor [56].

Structure	Study	Sensitivity (nm/RIU)	Range of λ	Medium/ RI	Comment	Ref
Gold-coated D-shaped PCF	Experimental and analytical	46,000	Vis-NIR	1.33–1.42	This is the maximum sensitivity. The average sensitivity of 9800 nm/RIU is reported	[54]
Silver-graphene, D-shaped PCF	Analytical	3700	Vis	1.33–1.37	This sensitivity is found for RI of 1.36	[61]
Two parallel Au-coated D-shaped PCFs	Analytical	13,500	NIR	1.27–1.33	13,500 is the maximum sensitivity for RI of 1.32	[62]
PCF externally coated with TiO_2-Au	Analytical	23,000	Vis-NIR	1.32–1.40	23,000 is the maximum sensitivity for RI of 1.32	[63]

Structure	Study	Sensitivity (nm/RIU)	Range of λ	Medium/ RI	Comment	Ref
PCF with Au-metalized microfluidic slots	Analytical	2000	Vis	1.33–1.34	The effect of geometrical parameters is studied. Sensitivity is inversely proportional to gold layer thickness	[64]
PCF with Au-coated multichannel	Analytical	2400	Vis	1.33–1.34	The effect of geometrical parameters is studied	[65]
Analyte filled with Au-coated core PCF	Analytical	2280	NIR	1.46–1.485	Several peaks were observed in the resonance spectrum	[66]

Table 3.
Characteristics of several reported PCF SPR sensors.

holes and the separation gap between them defines the light propagation characteristics of PCFs. These sensors own other advantages including small size and flexible structural design over conventional optical fiber and prism coupler SPR sensors. To date, numerous PCF SPR sensors have been demonstrated with different configurations. The schematics of some configurations are shown in **Figure 5**. **Figure 5a** shows the configuration in which the metal layer and the analyte are filled inside the cladding holes. External coatings and D shape PCF are shown in **Figure 5b** and **c** respectively.

The performance of recently reported PCF-based SPR sensors are compared in **Table 3**. Most of the reported sensors are based on theoretical and analytical studies. This is due to the fact that fabrication of these sensors requires a complex process.

5. Conclusion

In this review, the basic principles of SPR and various configurations of SPR excitation are reviewed. Since nanostructures of noble metals have tunable optical properties, they can be applied in nanoplasmonics-based devices and sensors. Nanoplasmonics has proven to be useful in sensing applications, especially for biological uses. Compared to SPR-based sensors, LSPR-based sensors exhibit unique properties, including higher sensitivities and figure of merits (FOM).

The researchers' aim to reduce the size of SPR- and LSPR-based sensors led to development of fiber-optic SPR-based sensors. The highest sensitivity reported in the literature allocates to PCF SPR sensors. They have shown their capability in providing high sensitivity as high as 46,000 nm/RIU [54] with respect to small RI changes. However, the majority of reported PCF SPR sensors are based on analytical studies (as it is shown in **Table 3**, most of the researches are only carried out with numerical simulations). This is due to complications of the fabrication process of the PCF SPR sensor. The complication mostly refers to interior metallic coating (into the core or cladding holes). Large interest in PCF SPR sensors among researchers increases the importance of the fabrication technique improvements.

IntechOpen

Author details

Parsoua A. Sohi and Mojtaba Kahrizi*
Department of Electrical and Computer Engineering, Concordia University, Montreal, Quebec, Canada

*Address all correspondence to: mojtaba.kahrizi@concordia.ca

References

[1] Lubbers DW, Opitz N. The pCO_2-/pO_2-optode: A new probe for measurement of pCO_2 or pO_2 in fluids and gases. Journal of Biosciences. 1975; **30**(7–8):532-533

[2] Kanso M, Cuenot S, Louarn G. Roughness effect on the SPR measurements for an optical fibre configuration: Experimental and. Journal of Optics A: Pure and Applied Optics. 2007;**9**:586-592

[3] SEO M, LEE J, LEE M. Grating-coupled surface plasmon resonance on bulk stainless steel. Optics Express. 2017;**25**(22):254-262

[4] Svedendahl M, Chen S, Kall M. An Introduction to Plasmonic Refractive Index Sensing. In: Dmitriev A, editor. Nanoplasmonic Sensors. Springer, NY: Integrated Analytical Systems. 2012. Available from: https://link.springer.com/chapter/10.1007/978-1-4614-3933-2_1

[5] Akowuah EK, Gorman T, Haxha S. Design and optimization of a novel surface plasmon resonance biosensor based on Otto configuration. Optics Express. 2009;**17**(26):491-496

[6] Rossi S, Gazzola E, Capaldo P, Borile G, Romanato F. Grating-coupled surface plasmon resonance (GC-SPR) optimization for phase-interrogation biosensing in a microfluidic chamber. Sensors. 2018;**18**(1621):1-13

[7] Gupta BD, Verma RK. Surface plasmon resonance-based fiber optic sensors: Principle, probe designs, and some applications. Journal of Sensors. 2009:1-12. DOI: 10.1155/2009/979761

[8] Zhang C, Li Z, Zhen S, Hui C, Cai S, Yu J. U-bent fiber optic SPR sensor based on graphene/AgNPs. Sensors and Actuators B: Chemical. 2017;**251**:127-133

[9] Ctyroky J et al. Theory and modelling of optical waveguide sensors utilising surface plasmon resonance. Sensors and Actuators B: Chemical. 1999;**54**(1–2): 66-73

[10] Dormeny AA, Sohi PA, Kahrizi M. Design and simulation of a refractive index sensor based on SPR and LSPR using gold nanostructures. Results in Physics. 2020;**16**:102869

[11] Fida F. Biosensing Based on Localized Surface Plasmon Resonance of Gold Nanostructures Fabricated by a Novel Nanosphere Lithography Technique. [Thesis]. Concordia University; 2008

[12] Prabowo BA, Purwidyantri A, Liu K-C. Surface plasmon resonance optical sensor: A review on light source technology. Biosensors. 2018;**8**(80):1-27

[13] Kretschmann E, Raether H. Radiative decay of non-radiative surface plasmon excited by light. Zeitschrift für Naturforschung A. 1968;**23**:2135-2136

[14] Roh S, Chung T, Lee B. Overview of the characteristics of micro- and nano-structured surface plasmon resonance sensors. Sensors. 2011;**11**(2):1565-1588

[15] Otto A. Excitation of nonradiative surface plasma waves in silver by the method of frustrated total reflection. Zeitschrift für Physik. 1968;**216**:398-410

[16] Allsop T, Neal R. A review: Evolution and diversity of optical fibre plasmonic sensors. Sensors. 2019; **19**(4874):1-19

[17] Petty CM. Molecular Electronics: From Principle to Practice. Wiley: United States; 2008

[18] Nguyen HH, Park J, Kang S, Kim M. Surface plasmon resonance: A versatile

technique for biosensor applications. Sensors. 2015;**15**:10481-10510

[19] Syahir A, Usui K, Tomizaki K, Kajikawa K, Mihara H. Label and label-free detection techniques for protein microarrays. Microarrays. 2015;**4**(2): 228-244

[20] Vollmer F, Arnold S. Whispering-gallery-mode biosensing: Label-free detection down to single molecules. Nature Methods. 2008;**5**(7):591-596

[21] Méjard R, Griesser HJ, Thierry B. Optical biosensing for label-free cellular studies. Trends in Analytical Chemistry. 2014;**53**:178-186

[22] Liedberg B, Nylander C, Lundstrm I. Biosensing with surface plasmon resonance—How it all started. Biosensors & Bioelectronics. 1995;**10**:1-9

[23] Liedberg B, Nylander C, Lunstrom I. Surface plasmon resonance for gas detection and biosensing. Sensors and Actuators. 1983;**4**:299-304

[24] Sathiyamoorthy K, Ramya B, Murukeshan VM, Wei Sun X. Modified two prism SPR sensor configurations to improve the sensitivity of measurement. Sensors and Actuators A: Physical. 2013; **191**:73-77

[25] Fida F, Varin L, Badilescu S, Kahrizi M. Gold nanoparticle ring and hole structures for sensing proteins and antigen–antibody interactions. Plasmonics. 2009;**4**:201-207

[26] Mock JJ, Hill RT, Tsai Y, Chilkoti A, Smith DR. Probing dynamically tunable localized surface plasmon resonances of film-coupled nanoparticles by evanescent wave excitation. Nano Letters. 2012;**12**:1757-1764

[27] Petryayeva E, Krull UJ. Localized surface plasmon resonance: Nanostructures, bioassays and biosensing—A review. Analytica Chimica Acta. 2011;**706**(1):8-24

[28] Tosi D, Poeggel S, Iordachita I, Schena E. Fiber optic sensors for biomedical applications. Opto-Mechanical Fiber Optic Sensors. 2018: 301-333. DOI: 10.1126/science.6422554

[29] Ekinci Y, Solak HH, Löffler JF. Plasmon resonances of aluminum nanoparticles and nanorods. Journal of Applied Physics. 2008;**104**(083107): 1-6

[30] Larsson EM, Alegret J, Ka M, Sutherland DS. Sensing characteristics of NIR localized surface plasmon resonances in gold nanorings for application as ultrasensitive biosensors. Nano Letters. 2007;**7**(5):1256-1263

[31] Movsesyan AR, Baudrion A-L, Adam P-M. Extinction measurements of metallic nanoparticles arrays as a way to explore the single nanoparticle plasmon resonances. Optics Express. 2018;**26**(5): 2949-2951

[32] Hao F, Larsson EM, Ali TA, Sutherland DS, Nordlander P. Shedding light on dark plasmons in gold nanorings. Chemical Physics Letters. 2008;**458**(4–6):262-266

[33] Wang S, Sun X, Ding M, Peng G. The investigation of an LSPR refractive index sensor based on periodic gold nanorings array. Journal of Physics D: Applied Physics. 2018;**51**(4):045101 (7pp)

[34] Canpean V, Astilean S. Multifunctional plasmonic sensors on low-cost subwavelength metallic nanoholes arrays. Royal Society of Chemistry. 2009;**9**(24):3574-3579

[35] Parsons J, Hendry E, Burrows CP, Auguié B, Sambles JR, Barnes WL. Localized surface-plasmon resonances in periodic nondiffracting metallic

nanoparticle and nanohole arrays. Physical Review B. 2009;**79**(7):1-4

[36] Chen Z, Li P, Zhang S, Chen Y, Liu P. Enhanced extraordinary optical transmission and refractive-index sensing sensitivity in tapered plasmonic nanohole arrays. Nanotechnology. 2019; **30**:335201(9pp)

[37] Bethe H. Theory of diffraction by small holes. Physical Review. 1944;**66** (7–8):163

[38] Hajiaboli A. Optical properties of thick metal nanohole arrays fabricated by electron-beam and nanosphere lithography. Physica Status Solidi A: Applications and Material Science. 2009;**206**(6668):976-979

[39] Rodrigo SG, de León-Pérez F, Martín-Moreno L. Extraordinary optical transmission: Fundamentals and applications. Proceedings of the IEEE. 2016;**104**(12):2288-2306

[40] Motogaito A, Morishita Y, Miyake H, Hiramatsu K. Extraordinary optical transmission exhibited by surface plasmon polaritons in a double-layer wire grid polarizer. Plasmonics. 2015;**10**(6):1657-1662

[41] Liu H, Lalanne P. Theory of the extraordinary optical transmission. Nature Letters. 2008;**452**:728-731

[42] Zhang J, Irannejad M, Yavuz M, Cui B. Gold nanohole array with sub-1 nm roughness by annealing for sensitivity enhancement of extraordinary optical transmission biosensor. Nanoscale Research Letters. 2015;**10**(238):1-8

[43] Liu S, Yang Z, Liu R, Li X. High sensitivity localized surface plasmon resonance sensing using a double split nanoring cavity. The Journal of Physical Chemistry C. 2011;**115**(50): 24469-24477

[44] Lee SY, Kim S-H, Jang SG, Heo CJ, Shim JW, Yang SM. High-fidelity optofluidic on-chip sensors using well-defined gold nanowell crystals. Analytical Chemistry. 2011;**83**(23): 9174-9180

[45] Bochenkov VE, Frederiksen M, Sutherland DS. Enhanced refractive index sensitivity of elevated short-range ordered nanohole arrays in optically thin plasmonic Au films. Optics Express. 2013;**21**(12):4428-4433

[46] Brian B, Sepúlveda B, Alaverdyan Y, Lechuga LM, Käll M. Sensitivity enhancement of nanoplasmonic sensors in low refractive index substrates. Optics Express. 2015; **17**(3):2335-2339

[47] Toderas F, Baia M, Baia L, Astilean S. Controlling gold nanoparticle assemblies for efficient surface-enhanced Raman scattering and localized surface plasmon resonance sensors. Nanotechnology. 2007;**18**: 255702

[48] Luther JM, Jain PK, Ewers T, Alivisatos AP. Localized surface plasmon resonances arising from free carriers in doped quantum dots. Nature Materials. 2011;**10**(4):361-366

[49] Sun Y, Xia Y. Increased sensitivity of surface plasmon resonance of gold nanoshells compared to that of gold solid colloids in response to environmental changes. Analytical Chemistry. 2002;**74**(20):5297-5305

[50] Im H, Sutherland JN, Maynard JA, Oh S. Nanohole-based surface plasmon resonance instruments with improved spectral resolution quantify a broad range of antibody-ligand binding kinetics. Analytical Chemistry. 2012;**84**: 1941-1947

[51] Lee KS, El-Sayed MA. Gold and silver nanoparticles in sensing and imaging: Sensitivity of plasmon

response to size, shape, and metal composition. Journal of Physical Chemistry B. 2006;**110**(39):19220-19225

[52] Jorgenson R, Yee S, Johnson K, Compton B. Novel surface-plasmon-resonance-based fiber optic sensor applied to biochemical sensing. In: Fiber Optics Sensors in Medical Diagonistics. 1993. pp. 35-48. DOI: 10.1117/12.144841

[53] Jorgenson R, Yee S. A fiber-optic chemical sensor based on surface plasmon resonance. Sensors and Actuators B: Chemical. 1993;**12**(3): 213-220

[54] Rifat AA, Ahmed R, Mahdiraji GA, Adikan FRM. Highly sensitive D-shaped photonic crystal fiber-based plasmonic biosensor in visible to near-IR. IEEE Sensors Journal. 2017;**17**(9):2776-2783

[55] Liu C et al. Numerical analysis of a photonic crystal fiber based on a surface plasmon resonance sensor with an annular analyte channel. Optics Communications. 2017;**382**:162-166

[56] Gangwar RK, Singh VK. Highly sensitive surface plasmon resonance based D-shaped photonic crystal fiber refractive index sensor. Plasmonics. 2017;**12**:1367-1372

[57] Piliarik M, Homola J. Surface plasmon resonance sensor based on a single-mode polarization-maintaining optical fiber. Sensors and Actuators B: Chemical. 2003;**90**:236-242

[58] Lin H-Y, Huang C-H, Cheng G-L, Chen N-K, Chui H-C. Tapered optical fiber sensor based on localized surface plasmon resonance. Optics Express. 2012;**20**(19):21693-21701

[59] Kim Y-C, Peng W, Banerji S, Booksh KS. Tapered fiber optic surface plasmon resonance sensor for analyses of vapor and liquid phases. Optics Letters. 2005;**30**(17):2218-2220

[60] Antohe I, Spasic D, Delport F, Li J, Lammertyn J. Nanoscale patterning of gold-coated optical fibers for improved plasmonic sensing. Nanotechnology. 2017;**28**:215301

[61] Dash JN, Jha R. On the performance of graphene-based D-shaped photonic crystal fibre biosensor using surface plasmon resonance. Plasmonics. 2015; **10**:1123-1131

[62] Wang F, Liu C, Sun Z, Sun T, Liu B. A highly sensitive SPR sensors based on two parallel PCFs for low refractive index detection. IEEE Photonics Journal. 2018;**10**(4):1-10

[63] Al Mahfuz M, Hossain MA, Haque E, Hai NH, Namihira Y, Ahmed F. A bimetallic-coated, low propagation loss, photonic crystal fiber based plasmonic refractive index sensor. Sensors. 2019;**19**(3794):1-12

[64] Akowuah EK et al. Numerical analysis of a photonic crystal fiber for biosensing applications. IEEE Journal of Quantum Electronics. 2012;**48**(11): 1403-1410

[65] Azzam SI, Hameed MFO, Shehata R, Heikal A, Obayya SS. Multichannel photonic crystal fiber surface plasmon resonance based sensor. Optical and Quantum Electronics. 2016;**48**(2):1-11

[66] Qin W, Li S, Yao Y, Xin X, Xue J. Analyte-filled core self-calibration microstructured optical fiber based plasmonic sensor for detecting high refractive index aqueous analyte. Optics and Lasers in Engineering. 2014;**58**:1-8